Mon. Not. R. Astron. Soc. **000**, 000–000 (0000) Printed 24 July 2014 (MN LATEX style file v2.2)

Stellar tidal disruption candidates found by cross-correlating the *ROSAT* Bright Source Catalogue and *XMM-Newton* observations

I. Khabibullin[1,2⋆], S. Sazonov[1,3]
[1]*Space Research Institute, Russian Academy of Sciences, Profsoyuznaya 84/32, 117997 Moscow, Russia*
[2]*Max-Planck-Institut für Astrophysik, Karl-Schwarzschild-Str. 1, 85740 Garching bei München, Germany*
[3]*Moscow Institute of Physics and Technology, Institutsky per. 9, 141700 Dolgoprudny, Russia*

Received 24 July 2014

ABSTRACT

We performed a systematic search for stellar tidal disruption events (TDE) by looking for X-ray sources that were detected during the *ROSAT* All Sky Survey and faded by more than an order of magnitude over the next two decades according to *XMM-Newton* serendipitous observations. Besides a number of highly variable persistent X-ray sources (like active galactic nuclei and cataclysmic variables), we found *three* sources that are broadly consistent with the TDE scenario: 1RXS J114727.1+494302, 1RXS J130547.2+641252, and 1RXS J235424.5-102053. A TDE association is also acceptable for the fourth source, 1RXS J112312.7+012858, but an AGN origin cannot be ruled out either. This statistics implies a TDE rate of $\sim 3\times10^{-5}$ yr^{-1} per galaxy in the Universe within $z \sim 0.18$, which is broadly consistent with the estimates of the TDE rate in the more local Universe obtained previously.

Key words: accretion, accretion discs – black hole physics – methods: observational – galaxies: nuclei.

1 INTRODUCTION

Tidal disruption of a star by a supermassive black hole (SMBH) is expected to be a rather rare event, taking place every 10^3 – 10^6 years in a typical galaxy in the local Universe (Wang & Merritt 2004). According to the canonical picture, some fraction (∼ 10%, Ayal, Livio, & Piran 2000) of the disrupted star's material should be captured and then accreted by the SMBH on a time-scale of about a year (Gurzadian & Ozernoi 1981; Rees 1988; Evans & Kochanek 1989; Phinney 1989; Ulmer 1999). This results in the formation of an accretion disc emitting quasi-thermally with the peak luminosity of 10^{43} – 10^{45} erg s^{-1}, mainly at extreme ultraviolet (EUV)/soft X-ray wavelengths (Strubbe & Quataert 2009). Thus, a previously EUV/X-ray faint galaxy can become active for some period of time, whilst the stellar debris are being accreted onto the SMBH, and then return to its initial quiescent state. Such tidal disruption events (TDE) can be searched for using repeated wide-area surveys spaced in time by at least a year (Sembay & West 1993; Komossa 2002; Gezari et al. 2009; van Velzen et al. 2011b; Stone, Sari, & Loeb 2013; Khabibullin, Sazonov, & Sunyaev 2014).

Only about a dozen TDE candidates have been identified so far (see Komossa 2012; Gezari 2012 for recent reviews), with the major contribution coming from X-ray observations (Komossa 2002; Donley et al. 2002; Esquej et al. 2008; Cappelluti et al. 2009; Maksym, Ulmer, & Eracleous 2010; Lin et al. 2011; Saxton et al. 2012; Maksym et al. 2013). The *ROSAT* All-Sky Survey (RASS, Voges et al. 1999) played the key role in the first X-ray identifications and provided a reference point for comparison with consequent *ROSAT* pointed observations (Komossa 2002; Donley et al. 2002) and later observations by *Chandra* and *XMM-Newton* (e.g. Esquej et al. 2008). Although up to several thousand TDEs had been expected to be detected during the RASS (Sembay & West 1993), only *five* were actually identified due to the lack of deep archival and timely follow-up X-ray observations needed for probing the pre- and/or post-outburst state (Komossa 2002; Donley et al. 2002). Therefore, plenty of TDEs will likely remain hidden in the RASS data at least until the forthcoming X-ray all-sky survey by the eROSITA telescope of the *SRG* observatory (eRASS, Khabibullin, Sazonov, & Sunyaev 2014).

Nevertheless, currently operating X-ray observatories have already covered a significant fraction of the sky with sensitivity at least ten times better than that of the RASS (∼ 3×10^{-13} erg s^{-1} cm^{-2} in the 0.5–2 keV energy band, Brandt & Hasinger 2005), thus providing an opportunity to search for TDEs that occurred during the RASS epoch (in 1990–1991) and have decayed since then. In the present study, we check all sources from the RASS Bright Source Catalogue (RASS-BSC, Voges et al. 1999) for a large (more than a factor of ten) flux decrease in *XMM-Newton* observations carried out between February 2000 and December 2012, which have covered ∼ 2% of the sky with a characteristic detection limit of ∼ 10^{-14} erg s^{-1} cm^{-2} in the 0.5–2 keV energy band.

⋆ E-mail: khabibullin@iki.rssi.ru

Similarly to the present work, Donley et al. (2002) looked for X-ray sources that occurred during the RASS. The difference is that we use the much deeper *XMM-Newton* serendipitous survey instead of *ROSAT* pointed observations for comparison with the RASS data. This allows us to search for fainter TDEs, down to the flux limit of RASS-BSC, in the fields observed by *XMM-Newton*. As a result, although the total area covered by *XMM-Newton* observations is much smaller than that covered by *ROSAT* pointed observations, we can probe the TDE rate out to a larger distance ($z \lesssim 0.2$) compared to Donley et al. (2002) while covering a similar volume of the Universe. Comparison of RASS and *XMM-Newton* data has previously been done by Esquej et al. (2008). However, their study was based on the *XMM-Newton* Slew Survey, whose sensitivity and sky coverage are similar to the survey constructed from *ROSAT* pointed observations, and it was aimed at flares that occurred during the *XMM-Newton* epoch and were undetected by the RASS. Due to the relatively small volume of the Universe probed by that study, it discovered only two TDE candidates, which nonetheless proved to be of high value thanks to their timely follow-up observations enabled by the accurate *XMM-Newton* localisations (Esquej et al. 2008).

In summary, with this study we aim to significantly increase the available sample of TDE candidates and to begin to find TDEs outside the local ($z < 0.1$) Universe. In the latter regard, the present study is similar to the much larger forthcoming *eROSITA* survey (Khabibullin, Sazonov, & Sunyaev 2014). An obvious drawback of the present study is the impossibility of follow-up observations of TDEs detected during the RASS due to their poor localisation and disappearance from the sky by the present day.

The outline of the paper is as follows. In Section 2 we review the databases and methods used in our analysis. A summary of the identified TDE candidates is presented in Section 3. In Section 4 we discuss the implications of this study for the TDE rate in the Universe. Some conclusions are provided in Section 5.

2 METHOD

Our study follows a number of previous searches for X-ray sources demonstrating a large amplitude flux drop (> 10) and a soft, approximately $\sim$ 0.05 keV blackbody, spectrum expected of TDEs (Komossa 2002; Donley et al. 2002; Esquej et al. 2008; Cappelluti et al. 2009; Maksym, Ulmer, & Eracleous 2010; Lin et al. 2011; Saxton et al. 2012; Maksym et al. 2013). Namely, we looked for sources that were bright in the RASS epoch and faded away over the next ~10–20 years, as revealed by serendipitous observations with *XMM-Newton*, since we do not expect any significant TDE-related emission at this very late phase.

2.1 ROSAT Bright Source Catalogue

The *ROSAT* All-Sky Survey Bright Source Catalogue (RASS-BSC) was constructed from the all-sky survey performed during the first six months of the *ROSAT* mission in 1990/91 (Voges et al. 1999). It contains 18,811 sources with a limiting count rate of 0.05 cts/s in the 0.1–2.4 keV energy band, which corresponds to at least 15 photons from a source. The typical positional accuracy is 30 arcsec and at a brightness limit of 0.1 cts/s (8,547 sources), the catalogue provides a sky coverage of 92%. The catalogue also provides the source extent, i.e. the amount by which the image of a source exceeds the point spread function, which could be used to distinguish extended and point sources.

The total energy band is divided in four channels: A(~0.1–0.4 keV), B(~0.5–2.0 keV), C(~0.5–0.9 keV) and D(~0.9–2.0 keV), and spectral characteristics are presented in the form of hardness ratios HR1=(CR(B)-CR(A))/(CR(B)+CR(A)) and HR2=(CR(D)-CR(C))/(CR(D)+CR(C)), where CR(X) is the count rate in a given channel X.

There are two standard methods for RASS-BSC (Voges et al. 1999) to convert measured count rates to the unabsorbed 0.1–2.4 keV flux, which differ in the assumptions about the source spectral shape. One assumes an absorbed power law with a fixed photon index $\Gamma = 2.3$, which is the typical value derived from *ROSAT* observations of extragalactic sources, and the absorbing column density fixed at the Galactic value along the given line of sight (Flux 1). The other approach (Flux 2) is based on the empirical relation for count rates and fluxes originally suited for stars (Voges et al. 1999). For these methods, the accepted detection limit of 0.05 cts/s translates to the following 0.1–2.4 keV flux limits for point sources: $Flux1 \sim 7 \times 10^{-13}$ erg s^{-1} cm^{-2} (assuming $N_H = 10^{20}$ cm^{-2}) and $Flux2 \sim 2 \times 10^{-13}$ erg s^{-1} cm^{-2} (for HR1=-1, see the conversion formula in Section 3.3.5 of Voges et al. 1999).

We make use of the FITS file with the catalogue available at the anonymous ftp-server ftp.xray.mpe.mpg.de[1]. The analysis was performed using standard general purpose tasks for the manipulation of FITS data contained in the the sub-package FUTILS of the HEASARC's FTOOLS package[2] (Blackburn et al. 1995).

2.2 XMM-Newton Serendipitous Source Catalogue

3XMM-DR4[3] is the third generation catalogue of X-ray sources serendipitously detected by the European Space Agency's *XMM-Newton* observatory. It follows the previous 2XMM catalogue (Watson et al. 2009, 2013).

The current version contains source detections drawn from 7427 *XMM-Newton* EPIC observations made between 2000 February 3 and 2012 December 8, covering a total of 794 deg^2 of the sky, accounting for overlaps. The position for a typical source can be determined with $\sim$ 2 arcsec accuracy (Watson et al. 2009). The median flux in the soft (0.2–2 keV) energy band is $\sim 6 \times 10^{-15}$ erg s^{-1} cm^{-2}, which is $\sim$ 100 times lower than the detection threshold accepted for RASS-BSC (see above).

In this study we are interested not only in X-ray sources detected by *XMM-Newton* but also in X-ray flux limits provided by *XMM-Newton* observations. Hence, we use the XMM flux upper limit server (FLIX[4]), which makes it possible, by scanning the *XMM-Newton* images corresponding to the 3XMM-DR4 catalogue, to estimate an upper limit on the X-ray flux from a given position as well as to measure the flux within a circle centred on that position.

2.3 Revealing decay of RASS-BSC sources with XMM-Newton observations

Our goal is to obtain a sample of TDE candidates by cross-correlating the RASS-BSC source catalogue with the *XMM-Newton* data. As usual in such studies, we should take both reliability and completeness of the resulting sample into account. We

[1] Or directly at ftp://ftp.xray.mpe.mpg.de/rosat/catalogues/rass-bsc/
[2] http://heasarc.gsfc.nasa.gov/ftools/
[3] http://xmmssc-www.star.le.ac.uk/Catalogue/xcat_public_3XMM-DR4.html
[4] http://www.ledas.ac.uk/flix/flix3

prefer to use a more reliable selection algorithm, since it is virtually impossible to perform follow-up observations to confirm or reject a TDE association for RASS sources.

As a first step, we leave only sources outside the Galactic plane, by requiring $|b| > 30^\circ$. There are two reasons for applying this constraint. First, the Galactic extinction at $|b| < 30^\circ$ is expected to significantly diminish the fluxes of TDE flares due to their soft X-ray spectra. Second, the increasing density of foreground Galactic sources (primarily cataclysmic variables) can cause significant contamination of the sample. However, the contribution of Galactic contaminant sources remains noticeable (∼50% of our raw candidate sample, see below) even for $|b| > 30^\circ$. In addition, we exclude sources with the angular extent larger than 30 arcsec, which allows us to avoid dealing with extended sources like galaxy clusters. Finally, we produce a list of positions that can be used as an input for the XMM flux upper limit server.

At the second stage, the XMM flux upper limit server reads the file produced previously and returns a FITS-file with fluxes in various energy bands measured within a circle centred on the RASS position of a given source, provided there are *XMM-Newton* observations of the corresponding field. We use the 0.2–2 keV energy band and an extraction radius of 60 arcsec, which exceeds the RASS localisation uncertainty, to obtain a conservative estimate. It is important to note that such a flux estimate will obviously include contributions from the background emission and from any sources falling into the extraction region. At energies above 1 keV, it is dominated by the nearly constant contribution of extragalactic sources with the total surface brightness of $4{\times}10^{-15}$ erg s^{-1} cm^{-2} arcmin $^{-2}$, while below 1 keV it is dominated by diffuse Galactic and local thermal-like emission, which varies from position to position and has the net surface brightness of the same order (Hickox & Markevitch 2006). Hence, we can miss potential TDE candidates located in highly crowded regions or regions polluted by extended sources. In addition, we remove *XMM-Newton* observations with very small exposure time and hence with a high uncertainty of the flux estimate.

Finally, we check whether the flux derived from the *XMM-Newton* observations is at least 10 times lower than the lowest of flux estimates provided by RASS-BSC (i.e. Flux1 or Flux2). This resulted in a preliminary sample of 24 TDE candidates, selected based on X-ray variability properties only. Since there are only ∼ 20 photons detected by *ROSAT* for each of these objects, we do not impose any additional constraints on our sample based on X-ray spectral properties of the sources (reflected in their hardness ratios, see Section 2.1).

We then additionally examined these candidate sources for any problems that might have significantly affected their positions and fluxes reported in RASS-BSC. To this end, we first checked for the presence of cautionary flags in RASS-BSC, which may reflect some difficulties met by the detection algorithm. In addition, we visually compared available RASS and *XMM-Newton* X-ray images for our candidates.

As a result, one candidate (1RXS J132654.5-271104), which is reported as displaying a complex diffuse emission pattern ('d'-flag) but nevertheless considered point-like in RASS-BSC, is likely associated with the Abell 1736 galaxy cluster. The flux reported in RASS-BSC is collected from a much larger region (roughly, from the extraction region with a radius of 5 arcmin) compared to the region (with a radius of 1 arcmin) we used to get an upper limit from *XMM-Newton* and can be dominated by X-ray emission from the intracluster medium.

A somewhat different situation takes place in two other cases, 1RXS J003406.7-020935 and 1RXS J012605.2-012151, where the regions of interest appear to be contaminated by both a relatively large number of point sources and relatively weak diffuse emission from RXC J0034.6-208 (a galaxy cluster candidate from Böhringer et al. 2004) and Abell 194, respectively, as is clearly seen on *XMM-Newton* images (see also Hudaverdi et al. 2006 reporting the results of *XMM-Newton* data analysis for Abell 194). In both cases, one of the brightest point sources in the field falls rather close to the centroid provided by RASS-BSC, albeit well outside the cited localisation uncertainty region. Namely, it is 3XMM J003410.7-021039 (IC 0029), with a 0.2–12 keV flux of $2.8{\pm}0.5\times10^{-13}$ erg/s/cm^2, 88 arcseconds away from the RASS-BSC centroid for 1RXS J003406.7-020935 (having 1σ localisation error of 15 arcseconds), and 3XMM J012600.6-012041 (the NGC547/NGC545 pair), with a 0.2–12 keV flux of $6.0{\pm}0.2\times10^{-13}$ erg/s/cm^2, 98 arcseconds apart from the RASS-BSC centroid for 1RXS J012605.2-012151 (having 1σ localisation error of 25 arcseconds). Assuming that it is these sources which are in fact responsible for the fluxes reported in RASS-BSC, these candidates then fail to satisfy our TDE selection criterion based on high-amplitude variability.

Thus, there remain 21 candidates in our sample. However, some of them still have cautionary RASS-BSC flags due to the presence of a nearby bright source, and we will discuss this specifically in every interesting case below.

2.4 Cross-correlation with other surveys

Since many of the RASS-BSC sources have been identified and classified since they were discovered, we searched NASA/IPAC Extragalactic Database[5] (NED) and the SIMBAD Astronomical Database[6] for possible identifications of our TDE candidates. *Nine* of the candidates turned out to be known stellar-type objects, including 7 systems with accreting white dwarfs (RX J0132.7-6554, Burwitz et al. 1997, EF Eri, Verbunt et al. 1997, RX J0527.8-6954, Trümper et al. 1991; Greiner et al. 1996a, RX J1039.7-0507, Appenzeller et al. 1998, WGA J1047.1+6335, Singh et al. 1995, RX J1957.1-5738, Thomas et al. 1996, RX J2022.6-3954, Burwitz et al. 1997), a symbiotic star, CD–43°14304 (Muerset, Wolff, & Jordan 1997), and a hot white dwarf, WD J2324-546 (Pounds et al. 1993).

Four other candidates have been reported to demonstrate signatures of the active galactic nucleus (AGN) activity: KUG 1624+351 – a Seyfert 1.5 (Sy1.5) galaxy at $z = 0.0342$ (Bade et al. 1998; Véron-Cetty & Véron 2006), RX J1225.7+2055 – a narrow line Seyfert 1 (NLSy1) galaxy at $z = 0.335$ (Greiner et al. 1996b), MCG -01-05-031 – a Seyfert 2 (Sy2) galaxy at $z = 0.0182$ (Panessa & Bassani 2002) and WPVS 007 – a NLSy1 galaxy at $z = 0.028$. The last object is famous for very unusual X-ray properties, primarily soft X-ray variability by two orders of magnitude over three years (Grupe et al. 1995) and has already been mentioned in the context of TDE searches (Donley et al. 2002). However, the very recent extensive monitoring of WPVS 007 by the *Swift* observatory clearly indicates a high level of short-term variability of the source consistent with a partial covering absorber model (Grupe et al. 2013). Having been observed by *XMM-Newton* for ∼ 100 kiloseconds (2010 June 11), the source was identified as 3XMM J003915.8-511701 with the mean 0.2–12 keV flux of

[5] http://ned.ipac.caltech.edu/
[6] http://simbad.u-strasbg.fr/simbad/

$(1.12 \pm 0.16) \times 10^{-14}$ erg s^{-1} cm^{-2}, i.e. $\sim$ 500 times fainter compared with the detection during the RASS. The other three sources have also been marginally detected by *XMM-Newton* and Table 1 provides brief information about these detections.

The remaining *eight* candidates (see Table 2 and Table 3) either do not have firm identification or are associated with galaxies with no obvious AGN signatures. We have looked for potential counterparts of these objects inside their *ROSAT* localisation regions using the Guide Star Catalog II (GSC-II)[7] based on the Digitized Sky Survey (DSS) images (Lasker et al. 2008), the Two Micron All Sky Survey (2MASS, Skrutskie et al. 2006)[8], the *Wide-field Infrared Survey Explorer* (*WISE*) all-sky survey[9] (Wright et al. 2010) and the Sloan Digital Sky Survey (SDSS)[10]. The next section presents the results of this search[11].

3 RESULTS

Table 2 summarizes the RASS-BSC data for the potential TDE candidates. Table 3 provides X-ray flux limits for these sources obtained more than 10 years later with *XMM-Newton*. Since the typical RASS localisation uncertainty is $r_{1\sigma} \sim 15$ arcsec, it is difficult to uniquely associate these TDE candidates with sources from IR, optical or high angular-resolution X-ray surveys, and we should regard all sources (if any) falling into the RASS localisation region as possible counterparts. We use the 2σ (i.e. $\approx$ 95%) confidence region (corresponding to a radius $r_{2\sigma} \approx 1.6 r_{1\sigma}$ for the two-dimensional Gaussian distribution) for such analysis. Hence, only a few per cent of true counterparts can be missed.

Typically, there are several possible counterparts in the RASS localisation region. For example, this is the case if SDSS photometric data are available. The easiest possibility of proceeding with identification in such cases is checking for sources with AGN or cataclysmic variable (CV) signatures and thus rejecting a TDE origin. This can be done in several ways. First, a TDE flare taking place in the RASS epoch is expected to disappear by the time of the *XMM-Newton* observations, while the X-ray emission from the TDE host (inactive) galaxy is very unlikely to exceed the *XMM-Newton* detection limit. In contrast, there can well be a significant X-ray detection in 3XMM-DR4 (of course, this flux being at least 10 times lower than the flux measured by *ROSAT*) in the case of an AGN or CV. Second, any spectral information could of course be helpful but, unfortunately, an optical spectrum is available only for a small fraction of the possible counterparts. Finally, WISE infrared (IR) colors can also indicate an AGN origin, and such information is indeed available for many of the possible counterparts.

In addition, we can put a simple, physically motivated constraint on the expected optical brightness of a TDE host galaxy. Indeed, given the mass of the central SMBH, M_{BH}, the (near) peak soft X-ray luminosity of a TDE is expected to be

$$L_X = kL_{Edd}(M_{BH}) = kL_{Edd,\odot}\frac{M_{BH}}{M_\odot}, \quad (1)$$

where $L_{Edd,\odot} \simeq 1.4 \times 10^{38}$ erg/s is the Eddington luminosity for one solar mass and the factor $k \sim 0.1$ accounts for the bolometric correction, possible geometrical dilution and the fact that the X-ray flux detected by RASS may be measured not exactly at the peak of the TDE (see e.g. Khabibullin, Sazonov, & Sunyaev 2014).

On the other hand, the optical luminosity of the TDE host galaxy could be roughly expressed as

$$L_V \simeq \frac{L_{V,bulge}}{P_b} \simeq \frac{200}{P_b} L_{V,\odot}\frac{M_{BH}}{M_\odot}, \quad (2)$$

where $L_{V,\odot} \simeq 4.6 \times 10^{32}$ erg/s is the solar V-band luminosity, $P_b \sim 0.1$ is the fraction of the bulge in the total galaxy luminosity[12], and we have converted $L_{V,bulge}$ to M_{BH} using the $M_{BH} - L$ relation from Gültekin et al. (2009) for $M_{BH} \sim 10^7 M_\odot$ (in fact, the $M_{BH} - L$ relation is almost linear, so the numerical factor in Eq. 2 depends on M_{BH} very weakly).

As a result, we obtain the following relation between the TDE soft X-ray (~0.2–2 keV) flux, F_X, and the optical flux of the host galaxy, F_V:

$$F_V = F_X\frac{L_V}{L_X} \simeq \frac{F_X}{k\,P_b}\frac{200\,L_{V,\odot}}{L_{Edd,\odot}} \simeq 0.064\frac{F_X}{k_1\,P_{b,1}}, \quad (3)$$

where $k_1 = k/0.1$ and $P_{b,1} = P_b/0.1$.

For $F_X = 3 \times 10^{-13}$ erg/s/cm^2, i.e. close to the RASS-BSC detection limit, $F_V = 1.9 \times 10^{-14}$ erg/s/cm^2, given $k = 0.1$ and $P_b = 0.1$, which translates to $m_V = 2.5(-5.5 - \log F_V) \simeq 20.55$. For $F_X = 1 \times 10^{-12}$ erg/s/cm^2, a typical flux for RASS-BSC sources (and for our candidate sources, see Table 2), one gets $m_V \simeq 19.25$. Thus, a TDE host galaxy is unlikely to be very faint, unless we deal with an outlier from the $M_{BH} - L_{V,bulge}$ relation. We caution though that the $M_{BH} - L_{V,bulge}$ correlation used above was derived from a sample with somewhat heavier SMBHs compared to those expected to produce most TDEs in the Universe.

Similar estimates can be done for the near-IR (e.g. K band) magnitude of TDE host galaxies. According to the $M_{BH} - L_K$ relation for the total (bulge+disk) K-band luminosity from Läsker et al. (2014),

$$L_K \simeq 300 L_{K,\odot}\frac{M_{BH}}{M_\odot} \quad (4)$$

for $M_{BH} \sim 10^7 M_\odot$[13], where $L_{K,\odot} \simeq 8 \times 10^{31}$ erg/s is the solar K-band luminosity (e.g. Binney & Merrifield 1998, which corresponds to a Vega magnitude $M_K = 3.28$). Therefore,

$$F_K = \frac{F_X}{k}\frac{300\,L_{K,\odot}}{L_{Edd,\odot}} \simeq 2 \times 10^{-3}\frac{F_X}{k_1}. \quad (5)$$

Hence, for $F_X = 1 \times 10^{-12}$ erg/s/cm^2, $F_K = 2 \times 10^{-15}$ erg/s/cm^2, or $m_K \simeq 19.4$[14].

For different classes of contaminating sources, yet simpler calculations can be carried out. As known from X-ray surveys, $0.1 \lesssim F_X/F_V \lesssim 10$ for AGN and CVs in the soft X-ray band (e.g. Maccacaro et al. 1988; Aird et al. 2010), which translates to $15.15 \lesssim m_V \lesssim 20.15$ given $F_X = 3 \times 10^{-13}$ erg/s/cm^2. Somewhat higher F_X/F_V ratios could be found during flares of luminous blazars (Maccacaro et al. 1988; Cenko et al. 2012). It should

[7] http://archive.eso.org/gsc/gsc
[8] http://www.ipac.caltech.edu/2mass
[9] http://irsa.ipac.caltech.edu/Missions/wise.html
[10] http://www.sdss3.org/
[11] The cross-correlation analysis was conducted mainly using the TOPCAT software (Taylor 2005).

[12] This value for P_b is typical for disk galaxies but not for elliptical ones. However, for elliptical galaxies M_{BH} typically exceeds the tidal disruption threshold for solar-type stars ($\sim 10^8 M_\odot$), so we do not expect significant contribution from such galaxies in our TDE sample.
[13] In this case, the $M_{BH} - L_K$ relation is also almost linear, so the numerical factor in Eq. 4 will be essentially the same for $M_{BH} \sim 10^6 M_\odot$.
[14] The flux-to-magnitude conversion was calculated as $m_K = 2.5(-6.95 - \log F_K)$, in accordance with the 2MASS photometric system (Cohen, Wheaton, & Megeath 2003).

Table 1. Strongly variable X-ray sources with AGN signatures

Name	Type[a]	z[a]	3XMM-DR4			RASS-BSC			Amplitude[d]
			3XMM ID	Date (UTC)	Flux[b]	Count rate[c]	Flux1[c]	Flux2[c]	
WPVS 007	NLSy1	0.028	J003915.8-511701	2010-06-11.9	1.12 ± 0.16	0.96±0.068	19.4	3.04	> 270
MCG -01-05-031	Sy2	0.0182	J014525.4-034938	2008-08-03.2	5.97±0.7	0.17±0.03	3.5	0.92	> 15
RX J1225.7+2055	NLSy1	0.335	J122541.9+205503	2003-06-12.7	9.95± 1.19	0.33±0.03	6.7	1.63	> 16
KUG 1624+351	Sy1.5	0.0342	J162636.5+350241	2007-08-17.1 2007-08-19.2	3.685± 0.708 3.61± 0.59	0.081±0.013	0.971	0.672	> 18 > 18

[a] See references in the text.
[b] The 0.2–12 keV flux as measured by *XMM-Newton*, 10^{-14} erg s^{-1} cm^{-2}.
[c] *ROSAT* count rate with a 1σ uncertainty (cts/s) and corresponding estimates for the 0.1–2.4 keV flux (Flux1 and Flux2, see text), 10^{-12} erg s^{-1} cm^{-2}.
[d] Estimated amplitude of the flux drop between the RASS-BSC and 3XMM-DR4 epochs. It is calculated relative to the lowest of Flux1 and Flux2, so the actual amplitude should be somewhat higher.

Table 2. RASS-BSC data for potential TDE candidates

1RXS ID	RA	Dec	PosErr[a]	CR[b]	eCR[b]	Exp[b]	HR1[c]	eHR1[c]	HR2[c]	eHR2[c]	Flux1[d]	Flux2[d]	N_H^e
J002048.5-253823	5.20208	-25.63986	16(26)	0.0563	0.0167	280	-0.32	0.27	-0.82	0.87	9.78	3.72	2.3
J005626.3-010615	14.10958	-1.10431	15(24)	0.0999	0.0202	312	0.65	0.18	0.61	0.19	21.5	11.7	3.4
J101326.2+061202	153.35918	6.20069	15(25)	0.0618	0.0154	434	-1	0.13	0	0	11.6	3.7	2.0
J112312.7+012858	170.80292	1.48292	17(28)	0.052	0.0143	375	0.08	0.27	0.15	0.35	13.7	4.53	3.5
J114727.1+494302	176.86292	49.71722	9(15)	0.414	0.0402	299	-0.97	0.02	1	1.3	63.3	13.1	1.7
J130547.2+641252	196.44666	64.21445	9(15)	0.167	0.0207	544	-0.82	0.06	-0.62	0.28	23.2	6.61	1.5
J215101.5-302852	327.75626	-30.48111	14(23)	0.0534	0.0159	333	-0.34	0.24	0.42	0.47	8.29	3.47	1.7
J235424.5-102053	358.60208	-10.34806	24(39)	0.0523	0.0153	310	1	0.25	-0.13	0.29	10.8	7.12	2.7

[a] 1σ localisation uncertainty and corresponding radius of the 95% confidence region, arcsec.
[b] The source mean count rate and corresponding 1σ error (both in units of counts s^{-1}) and exposure time (in sec).
[c] Hardness ratios (see text) with corresponding 1σ errors.
[d] 0.2–2.4 keV flux estimates (see text), 10^{-13} erg s^{-1} cm^{-2}.
[e] Total Galactic H I Column Density (divided by 10^{20} cm^{-2}) as determined with the *nH* utility of the *FTOOLS* package (based on the map of Kalberla et al. 2005).

be mentioned however that in the case of AGN and CVs, optical counterpart emission can be variable and tightly related to the X-ray emission. So if we compare the (relatively high) X-ray flux measured during the RASS with non-contemporaneous optical observations (e.g. SDSS), the resulting X-ray/optical flux ratio may be different, likely higher, than estimated above, hence the optical counterpart may be somewhat fainter.

For flaring stars, $F_X/F_V \sim 10^{-3}$–10^{-2} is much more typical (with rare exceptions of very intense flares in low-mass stars, Favata & Micela 2003[15]), so the optical counterpart is expected to be brighter than $m_V \simeq 13$ in this case.

In summary, the optical counterparts of our candidate sources are likely to be present in the SDSS photometric data (complete to $r \sim 22.2$, Abazajian et al. 2004), if available, even in the case of AGN/CV association, and they are probably sufficiently bright to be present in DSS images in the case of TDE association (GSC-II is complete to $R_F \simeq 20$, Lasker et al. 2008).

3.1 1RXS J002048.5-253823

1RXS J002048.5-253823 is located approximately 5 arcminutes from the galaxy cluster Abell 022, which is present in RASS-BSC as an independent X-ray source, 1RXS J002041.8-254307, and is ~ 6 times brighter than 1RXS J002048.5-253823. Therefore, the localisation and the flux estimate could be somewhat biased for 1RXS J002048.5-253823. However, examination of the RASS image shows that the two sources are well separated from each other. The available crude spectral information (hardness ratios), HR1=−0.32 ± 0.27 and HR2=−0.82 ± 0.87 for 1RXS J002048.5-253823 against HR1=−0.31±0.14 and HR2=−0.22±0.15 for 1RXS J002041.8-254307, is of little value in this respect given the large uncertainties for the fainter source.

Moreover, there is a faint 3XMM-DR4 source (3XMM J002049.3-253828) with the 0.2–2 keV flux of (1.7±0.5)×10^{-14} erg/s/cm^2, i.e. close to the detection limit of the 3XMM-DR4 catalogue, inside the 1σ-region (12 arcsec away from the reported RASS-BSC centroid). This source has an optical counterpart in the DSS image (and the corresponding entry in GSC-II with R_F = 17.1), a near-infrared counterpart in the 2MASS catalogue and a mid-infrared counterpart in the *WISE* catalogue (see Fig. 1 and Table 4). The *WISE* colors (namely, $W2 - W1 = 1.24 > 0.8$) strongly indicate an AGN association for this source (Stern et al. 2012). Since there are no other objects inside the RASS localisation region, we suggest that 1RXS J002048.5-253823 is a high-amplitude

[15] See also Section 6.5 in Merloni et al. (2012) for a relevant discussion.

Table 3. XMM-Newton flux limits for potential TDE candidates

1RXS	XMM ObsID	OffAxis[a]	Date	Exposure, s	Flux limit[b]	Ratio1[c]	Ratio2[c]
J002048.5-253823	201900301	4.386714	2004-05-26	9160	2.3 ± 0.3	43	16
	12440101	13.3243	2001-01-15	7711	3.1 ± 0.8	70	38
J005626.3-010615	402190501	8.833312	2006-06-16	6270	5.9 ± 1.8	37	20
	505211001	8.702417	2007-07-15	4905	3.6 ± 1.0	60	33
J101326.2+061202	600920301	4.105885	2009-05-26	4337	2.8 ± 0.5	41	13
J112312.7+012858	145750101	7.475069	2003-06-23	9966	5.4 ± 0.4	25	8.4
J114727.1+494302	604020101	1.638498	2009-11-21	1632	1.6 ± 0.7	410	84
J130547.2+641252	151790701	1.726202	2003-10-10	4456	0.4 ± 0.9	560	160
J215101.5-302852	103060401	10.47006	2001-05-01	7341	4.2 ± 0.6	20	8.2
J235424.5-102053	108460301	5.601944	2001-06-20	11009	1.1 ± 0.5	96	63

[a] Offset of the candidate RASS-BSC source (the first column) from the centre of the *XMM-Newton* field of view during a given observation (specified in the second column), arcmin.
[b] Estimated 0.2–2 keV flux within the 60 arcsec-radius region around the RASS-BSC position, with a 1σ uncertainty, 10^{-14} erg/s/cm^2. Note that this flux includes the background contribution.
[c] *ROSAT/XMM-Newton* flux ratio, found by comparison with the Flux1 or Flux2 estimate for RASS-BSC (see Table 2).

Figure 1. The Digitized Sky Survey (DSS) image (2'x2') of the region around 1RXS J002048.5-253823. The dashed and solid blue circles confine the 1σ and 2σ regions around the centroid of the *ROSAT* source, respectively. Red squares mark 2MASS sources, green crosses mark 3XMM sources (if any). For those fields with SDSS data available (see the subsequent figures), black diamonds mark the positions of SDSS sources. The arrow points out the most probable counterpart.

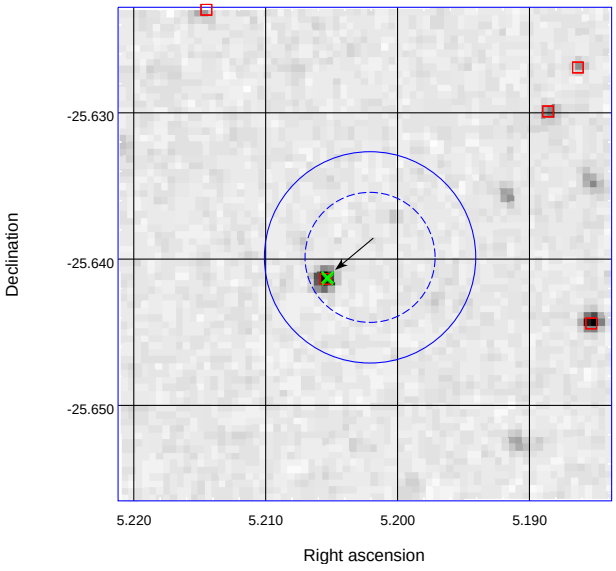

($\gtrsim 50$ if Flux1 is used as a flux estimate for the RASS-epoch) AGN flare.

We conclude that 1RXS J002048.5-253823 is probably not a TDE.

3.2 1RXS J005626.3-010615

This candidate is also located nearby a galaxy cluster, Abell 119, though approximately 10 arcminutes from its centre. Abell 199 enters RASS-BSC as 1RXS J005617.5-011501, being ~ 5 times brighter than 1RXS J005626.3-010615 with the extension of $\gtrsim 2$ arcmin. So, the sources seem to be well separated for the extraction region of the fainter one (10 arcmin in diameter) to include almost no extended emission from the brighter one. Both hardness ratios are also formally different for them: HR1=0.65 ± 0.18, HR2=0.61±0.19 for 1RXS J005626.3-010615 against HR1=0.88± 0.05, HR2=0.29 ± 0.08 for 1RXS J005617.5-011501.

There are seven SDSS sources inside the localisation region (see Fig. 2). All of them are faint, $r \gtrsim 20$, and thus invisible in the DSS image. An optical spectrum is available for only one source, which can be unambiguously classified as an M-star. This source (24 arcsec from the RASS centroid) is also the only one with a 2MASS counterpart. Although such a star could potentially produce an intense X-ray flare, it should be much brighter since the X-ray flux in the *ROSAT* energy range exceeded 10^{-12} erg/s/cm^2 and one should then expect $m_V \lesssim 16.5$ assuming $F_X/F_V \lesssim 1$ (such ratios correspond to the most extreme stellar flares).

Three other sources are identified as extended ones and another three are consistent with being point-like. The data on these sources are given in Table 4. An extended source 16 arcsec away from the RASS-BSC centroid is the only one detected by *WISE* and its colors favour an AGN association. It is also the optically brightest one with $r \approx 21.0$. This object can thus be considered the most probable counterpart. As to its nature, it could be a highly variable AGN (perhaps a blazar) with a very high F_X/F_V ratio.

We thus conclude that 1RXS J005626.3-010615 is unlikely to be a TDE.

3.3 1RXS J101326.2+061202

There are two SDSS sources at the boundary of the localisation region, 25 arcsec away from the RASS-BSC centroid (see Fig. 3). One is classified as a K star according to the SDSS spectrum, so it potentially could be responsible for the highly variable X-ray emission. Indeed, the optical magnitudes of the source satisfy the $F_X/F_V \lesssim 1$ condition discussed above. This source is also the only one inside the uncertainty region with 2MASS (with JHK magnitudes of 15.56, 14.86 and 14.82) and WISE (with $W1$ = 14.69 and

Figure 2. DSS image (2'x2') of the region around 1RXS J005626.3-010615. The symbols are the same as for Fig. 1.

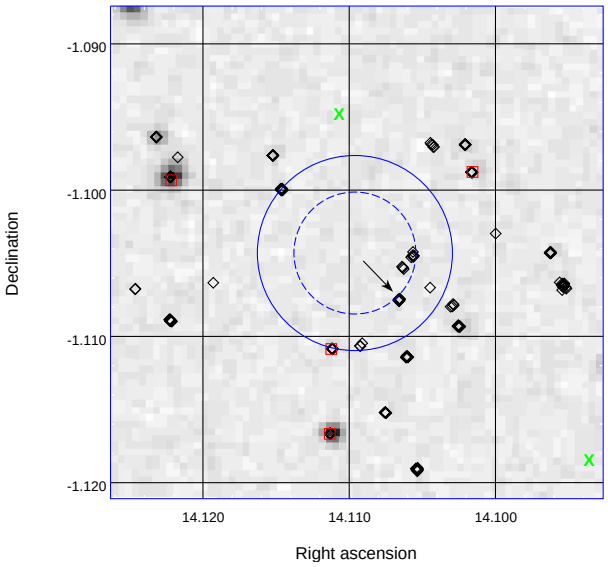

Figure 3. DSS image (2'x2') of the region around 1RXS J101326.2+061202. The symbols are the same as for Fig. 1.

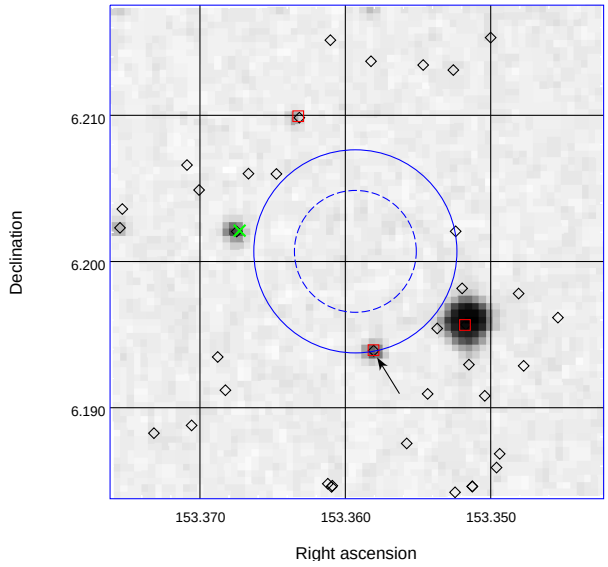

$W2 = 14.79$) counterparts. The other source is too faint to even be considered a possible counterpart in the case of a TDE association (see Table 4). Thus, we suggest that the most probable counterpart is the K star, which experienced a strong flare during the RASS.

We conclude that 1RXS J101326.2+061202 is unlikely to be a TDE.

Figure 4. DSS image (2'x2') of the region around 1RXS J112312.7+012858

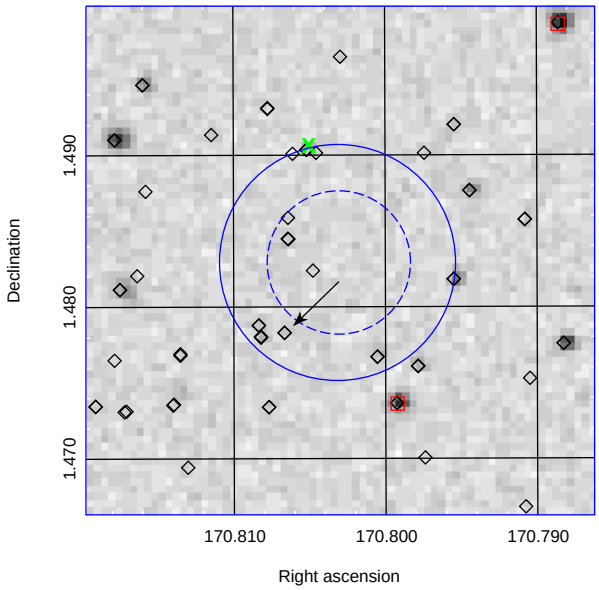

3.4 1RXS J112312.7+012858

There is a 3XMM-DR4 source (3XMM J112313.1+012924), with a flux of $(6.0 \pm 0.8) \times 10^{-14}$ erg/s/cm^2 in the 0.2–2 keV energy band, at the boundary of the localisation region (28 arcsec from the RASS-BSC centroid). This source has a faint, non-extended SDSS counterpart with (22.2, 21.3, 21.0, 21.4, 20.8) *ugriz* magnitudes, but there are no 2MASS or *WISE* counterparts. Taking these facts together, we consider association of the 3XMM-DR4 source with 1RXS J112312.7+012858 unlikely.

In total, there are eleven SDSS sources inside the localisation region. One of these has been confidently identified as an A0 star by means of optical spectroscopy. The data on all other sources are summarized in Table 4. The brightest SDSS object ($r = 19.9$), 21 arcsec away from the RASS-BSC centroid, is consistent with an extended source and is also the only one with a *WISE* counterpart. The first *WISE* color ($W1 - W2 = 15.114 - 14.831 = 0.283$) makes a luminous AGN association unlikely for this source. However, this object can be the host galaxy of a TDE.

We conclude that 1RXS J112312.7+012858 is possibly a TDE.

3.5 1RXS J114727.1+494302

This source, also known as RBS 1032, has been intensively investigated by Ghosh et al. (2006). They reported an ultrasoft X-ray spectrum, consistent with a blackbody with $\kappa T_{bb} \simeq 70$ eV, as well as a $\sim$ 3-fold flux drop from the original RASS detection (November 05, 1990) to the first pointed *ROSAT* observation carried out $\sim$ 2.1 years later (December 07, 1992) and a $\sim$ 6-fold drop to the second pointed observation $\sim$ 3.6 years later (June 05, 1994) (Ghosh et al. 2006). The authors identified RBS 1032 with a dwarf spheroidal galaxy (SDSS J114726.69+494257.8) at $z = 0.026$ with no optical signatures of nuclear activity. The *WISE* colours of this source

($W1 - W2 = 0.115$) also rule out a luminous AGN. *XMM-Newton* detected only a marginal signal from this position in late 2009 with the net 0.2–12 keV flux of $(1.1 \pm 0.6) \times 10^{-14}$ erg s^{-1} cm^{-2}.

There are two other SDSS extended sources inside the localisation region, with neither 2MASS nor *WISE* detection (see Fig. 6 and Table 4). These sources are too faint to be considered potential TDE hosts.

Ghosh et al. (2006) argued that the variable X-ray emission may come from an intermediate mass black hole accreting matter from a white dwarf companion. The estimated soft X-ray luminosity at peak is $\sim 10^{43}$ erg/s/cm^2 and fitting the X-ray spectra with a blackbody model yields a temperature of $\kappa T_{bb} \simeq 70$ eV (Ghosh et al. 2006). Both of these characteristics are consistent with the TDE scenario (Komossa 2002; Esquej et al. 2008). However, the six-fold flux decrease in the 3.6 years spanned by the *ROSAT* observations may seem to be too small for the TDE scenario assuming that the first detection occurred near the TDE peak.

However, the estimated luminosity is not sufficiently high to exclude the possibility that the first detection in fact occurred at a relatively late phase of the event. Indeed, assuming the canonical shape of the decay phase of the TDE light curve (Phinney 1989),

$$\frac{L(\tau+\delta t)}{L(\tau)} = \left(\frac{\tau+\delta t}{\tau}\right)^{-5/3}, \qquad (6)$$

where τ is the time of the RASS observation relative to the disruption moment and $\delta t = 3.6$ yrs is the time passed between the RASS observation and the second pointed *ROSAT* observation. Given that the unabsorbed 0.1–2.4 keV flux decreased from 6.0×10^{-12} erg s^{-1} cm^{-2} to 1.1×10^{-12} erg s^{-1} cm^{-2} during this period (Ghosh et al. 2006), we find $L(\tau+\delta t)/L(\tau) = 1.1/6.0$, so $\tau \simeq 2.0$ yrs. This implies that the disruption took place near the 5th of November, 1988. Since the duration of the early (Eddington-limited) phase $\tau_{Edd} \simeq 0.25\,(M_{BH}/10^7 M_\odot)^{2/5}$ for the minimal peri-center distance, $R_p = 3R_S$ (with $R_S = 2GM_{BH}/c^2$ being the Schwarzschild radius of the black hole), of the disrupted star (e.g. Strubbe & Quataert 2009), the peak luminosity is expected to be as high as $L_{peak} \simeq 30L(\tau) \simeq 3\times10^{44}$ erg/s for $M_{BH} = 10^7 M_\odot$, which is nonetheless ~5 times smaller than the Eddington luminosity for this black hole mass. The same calculation for $M_{BH} = 5\times10^6 M_\odot$ ($\tau_{Edd} \simeq 0.19$ yr) results in $L_{peak} \simeq 50L(\tau) \simeq 5\times10^{44}$ erg/s, i.e. just slightly below the corresponding Eddington luminosity. Although these estimates may be slightly affected by the bolometric correction, which can be estimated as $L_{bol} \simeq 1.1L_{X,0.1-2.4}$ from the observed shape of the spectrum (a black body with $\kappa T_{bb} = 70$ eV), and geometrical effects, it appears that values $M_{BH} \lesssim 5\times10^6 M_\odot$ are unlikely.

Therefore, the X-ray light curve seems to be consistent with a TDE that occurred near a 'normal' SMBH with $M_{BH} = 5\times10^6 - 10^7 M_\odot$, even though a simple power-law model predicts an order of magnitude higher flux for the *XMM-Newton* epoch (see Fig. 5 for an illustration) – this is in fact not surprising since at this very late stage of the TDE flare the feeding rate of the SMBH is expected to have fallen by several orders of magnitude.

We note that for $M_{BH} = 5\times10^6 - 10^7 M_\odot$, one could expect a somewhat lower temperature of the multicolour blackbody accretion disk, $\kappa T_{bb} \simeq 40 - 50$ eV $\propto M_{BH}^{-1/4}$ (Shakura & Sunyaev 1973). However, at late phases (as suggested here for the *ROSAT* observations) when the luminosity is as low as a few percent of the the peak value, i.e. the mass accretion rate is a few per cent of the critical accretion rate, the X-ray spectrum may harden due to transition to an inefficiently cooling accretion flow and/or formation of relativistic jets.

Therefore, 1RXS J114727.1+494302=RBS 1032 is probably a tidal disruption event associated with a SMBH of mass $M_{BH} \sim 5\times10^6 - 10^7 M_\odot$, which was caught by *ROSAT* at a fairly late phase. We note however that the inferred black-hole mass may be too high for the dwarf host galaxy of RBS 1032 (Ghosh et al. 2006).

Figure 5. An example of fitting the long-term X-ray light curve (the fluxes measured during the RASS and two subsequent pointed *ROSAT* observations of RBS 1032 by a power-law decay, i.e. $f \propto \left(\frac{t-t_0}{\tau_{Edd}}\right)^{-5/3}$, where t_0 is the disruption moment, for two values of the duration of the Eddington-limited phase $\tau_{Edd} = 0.19$ and 0.25 yr (thick blue and red lines, respectively. The corresponding peak fluxes and luminosities (right axis, for the luminosity distance to the source $d_L = 114$ Mpc) are marked by the solid blue and dashed red lines. Also shown is the marginal detection of the source by *XMM-Newton* in late 2009, which demonstrates a strong flux drop after ~ 20 years.

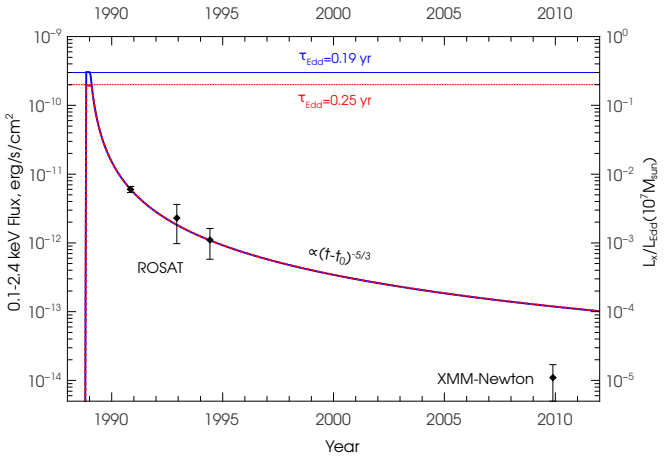

Figure 6. DSS image (2'x2') of the region around 1RXS J114727.1+494302

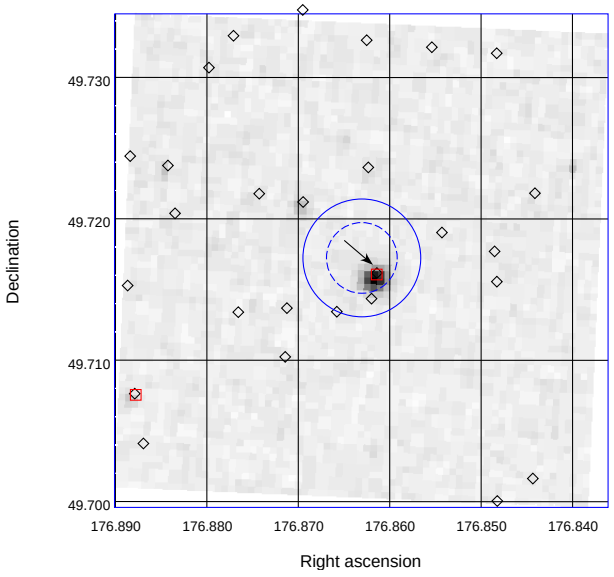

Figure 7. DSS image (2'x2') of the region around 1RXS J130547.2+641252

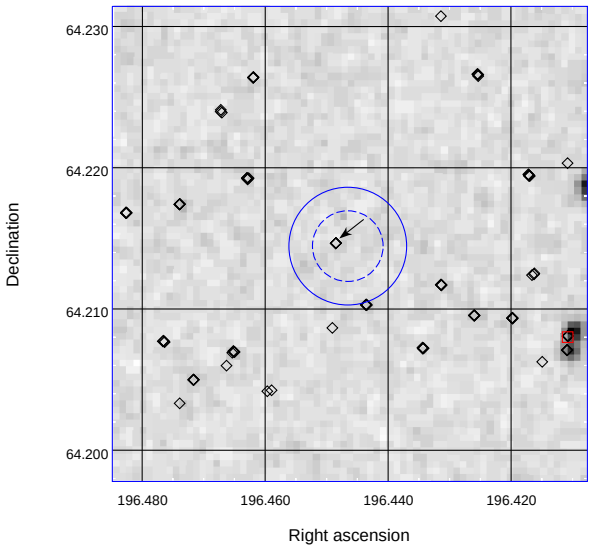

Figure 8. DSS image (2'x2') of the region around 1RXS J215101.5-302852.

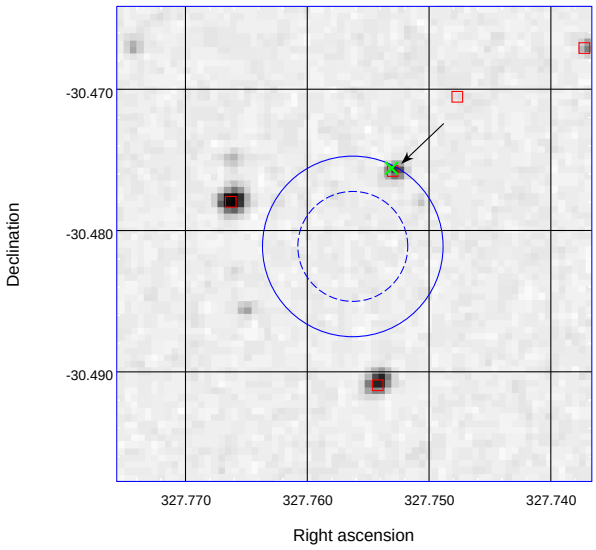

3.6 1RXS J130547.2+641252

There is only one SDSS source inside the localisation region (3 arcsec away from the RASS-BSC centroid, see Fig. 7). It is consistent with an extended source and has (22.5, 22.0, 20.9, 20.6, 20.4) *ugriz* magnitudes. This object is fainter than would be expected for a TDE host galaxy, albeit not very dramatically.

We conclude that 1RXS J130547.2+641252 is possibly a TDE.

3.7 1RXS J215101.5-302852

A weak 3XMM-DR4 source (3XMM J215100.7-302832), $(4.1 \pm 0.8) \times 10^{-14}$ erg/s/cm^2 (0.2–2 keV), is detected at the boundary of the localisation region (22 arcsec from the RASS-BSC centroid). This source has an optical counterpart in the DSS image (with $R_F = 18.6$ for the corresponding entry in GSC-II) as well as infrared counterparts in the 2MASS (with *jhk* magnitudes of 16.849, 16.304 and 15.347) and *WISE* (with $W1, W2, W3$ magnitudes of 13.985, 12.949 and 10.192) surveys (see Fig. 8). The first *WISE* colour, $W1 - W2 = 1.036$, strongly indicates an AGN origin.

We conclude that 1RXS J215101.5-302852 is unlikely to be a TDE.

3.8 1RXS J235424.5-102053

1RXS J235424.5-102053 is located approximately 5 arcminutes from the centre of the galaxy cluster Abell 2670. The latter enters RASS-BSC as 1RXS J235409.4-102506, is ~ 10 times brighter than 1RXS J235424.5-102053 and has an angular extent of ~ 1.5 arcmin. The uncertainties in the hardness ratios for 1RXS J235424.5-102053 are too large to draw any conclusions based on them. We note however that the corresponding spectrum should be rather peculiar with HR1=1.0±0.25, i.e. having no counts in the 0.1–0.4 keV energy channel, and HR2=-0.13±0.29 (while 1RXS J235409.4-102506 has HR1=0.83 ± 0.06 and HR2=0.24 ± 0.1).

The most prominent candidate for the counterpart of this source is a bright SDSS galaxy (17 arcsec away from the RASS-BSC centroid, see Fig. 9) at $z = 0.0805$, which may be a distant member of the Abell 2670 cluster ($z = 0.076$). Its optical spectrum does not show signatures of luminous nuclear activity, which is confirmed by the colours of the corresponding *WISE* counterpart ($W1 - W2 = 0.0$). All other eight SDSS sources inside the localisation region are faint ($r > 20$) and not detected by *WISE*. We further note that the bright SDSS galaxy appears to be a disk one observed nearly edge-on, which might cause significant absorption of the X-ray emission in the softest energy band of *ROSAT* and thus explain the measured value of HR1 close to unity.

We conclude that 1RXS J235424.5-102053 could still be considered a possible TDE candidate. However, we cannot exclude that it is a spurious point-like source on a RASS image contaminated by extended cluster emission.

4 DISCUSSION

Since any TDEs that may be present in our sample occurred almost 25 years ago, there is not much that can be done to explore their individual properties (see e.g. Bower et al. 2013 who looked for the late-time radio emission from TDE candidates discovered during the RASS). Nonetheless, this sample is valuable for studying TDE population properties. In particular, it allows us to put a constraint on the rate of TDEs in the local Universe.

4.1 Comparison with the results of Donley et al.

We first compare our results with the findings of Donley et al. (2002). Their sample was limited to relatively bright X-ray sources, with the unabsorbed 0.2–2.4 keV flux during the RASS higher than $f_0 = 2 \times 10^{-12}$ erg/s/cm^2 (assuming a power-law spectrum with $\Gamma = 4$), which was due to the sensitivity threshold of the subsequent *ROSAT* pointed observations (Donley et al. 2002) used in the

Table 4. Possible counterparts of potential TDE candidates. The coordinates of the most probable counterparts are marked in boldface.

Candidate	Counterpart							
	RA	Dec	Dist[a]	WISE, $W1–W2$ [b]	2MASS, JHK_s	SDSS, Class ($ugriz$)[c]	3XMM[d]	Nature
1RXS J002048.5-253823	**5.2054**	**-25.6414**	12	13.3–12.1	16.5–16.1–15.0	s(17.33,17.32,17.74)[e]	1.68± 0.46	AGN
	14.1057	-1.1045	13			s(25.0,23.5,22.6,22.3,22.5)		
	14.1063	-1.1053	13			g(22.5,22.2,21.7, 22.0,21.0)		
	14.1066	**-1.1075**	16	16.8–15.7		g(22.3,21.9,21.0,20.4,20.1)		AGN
1RXS J005626.3-010615	14.1045	-1.1067	20			s(22.6,25.4,24.3,24.3,23.0)		
	14.1093	-1.1106	23			s(23.4,24.0,22.8,22.9,21.6)		
	14.1146	-1.1000	24			g(23.9,24.3,22.5,21.4,20.9)		
	14.1110	-1.1108	24	14.8–14.6	15.8–15.1–14.9	s(22.6,21.8,20.1,18.3,17.3)		M-star
1RXS J101326.2+061202	**153.3579**	**6.1939**	25	14.7–14.8	15.6–14.9–14.8	s(21.4,18.7,17.4,17.0,16.7)		K-star
	153.3523	6.2021	25			s(24.6,24.0,24.1,22.6,22.1)		
	170.8046	1.4824	7			s(23.2,22.5,21.9,22.0,22.0)		
	170.8063	1.4845	13			g(22.0,22.4,21.6,20.3,19.8)		
	170.8063	1.4859	16			g(25.2,23.2,23.6,21.9,21)		
	170.8065	**1.4783**	21	15.1–14.8		g(24.1,21.6,19.9,19.2,18.8)		TDE
	170.8004	1.4767	24			s(22.4,22.1,21.7,21.4,21.1)		
1RXS J112312.7+012858	170.8082	1.4788	24			s(24.4,22.9,21.3,20.7,20.3)		
	170.8081	1.4781	26			g(21.6,21.4,20.7,20.5,21.5)		
	170.8044	1.4902	27			g(24.6,25.5,23.6,21.8,22.0)		
	170.7954	1.4818	27			s(21.3,20.5,20.2,20.0,20.0)		
	170.8050	1.4903	28			s(22.2,21.3,21.0,21.4,20.8)	6.0 ± 0.8	AGN/CV?
	170.8060	1.4901	28			s(25.1,25.4,25.5,21.9,23.0)		
	176.8613	**49.7161**	6	14.5–14.3	15.9–15.1–15.2	g(19.1, 17.7,17.1,16.8,16.6)		TDE(z=0.026)
1RXS J114727.1+494302	176.8618	49.7143	11			g(23.9, 23.7,22.7,23.2,22.0)		
	176.8656	49.7133	15			g(22.7, 22.7,22.4,23.1,23.9)		
1RXS J130547.2+641252	**196.4486**	**64.2145**	3			g(22.5,22.0,20.9,20.5,20.4)		TDE
1RXS J215101.5-302852	**327.7528**	**-30.4758**	22	14.0–13.0	16.8–16.3–15.3	g(18.34,18.56,17.74)[e]	4.1 ± 0.8	AGN
	358.6027	-10.3484	2			s(24.8, 23.6,21.8,20.9,20.3)		
	358.6047	-10.3501	12			g(22.7,23,21.7,21.5,21.7)		
	358.6017	-10.3446	13			s(21.4,20.8,20.9,21,21.2)		
	358.5976	**-10.3467**	17	13.7–13.7	15.4–14.7–14.3	g(19.6,17.7,16.8,16.4,16)		TDE?(z=0.081)
1RXS J235424.5-102053	358.6036	-10.3538	21			g(23.1,21.8,20.8,20.8,20.8)		
	358.5976	-10.3542	28			s(23,22.8,22.2,22.3,22.6)		
	358.597 3	-10.3542	28			g(23.6,22.7,22.1,22.3,22)		
	358.609 3	-10.3542	33	17.0–16.5		g(23.7,22.3,22,21.1,20.6)		
	358.6003	-10.3578	36	16.8–16.8		g(23.5,22.4,22.3,21,20.8)		

[a] Distance from the centroid of the RASS-BSC localisation, arcsec.
[b] *WISE* photometry becomes unreliable at approximately $W1 = 14$, $W2 = 13.5$. Values $W3 > 12$ (as is typical of the detections under consideration) should be regarded as marginal detections, hence we make no use of the $W3$ magnitude in our analysis (see text).
[c] A source type (*s* for stellar-like and *g* for galaxy-like) is given along with the *ugriz* magnitudes.
[d] The X-ray (0.2–2 keV) flux of the source in the 3XMM-DR4 catalogue, 10^{-14} erg s^{-1} cm^{-2}.
[e] DSS data is provided if no SDSS data is available: type (*s* for point-like and *g* for an extended source) and (B_J, R_F, I_N) magnitudes, taken from the second generation Guide Star Catalog (Lasker et al. 2008). The characteristic uncertainty for these photometric magnitudes is ≈ 0.2 for sources at high ($|b| > 30°$) galactic latitudes (Lasker et al. 2008).

analysis for demonstrating that the flux of a given RASS source has undergone a strong decline. Since we use the more sensitive *XMM-Newton* observations for the same purpose, our resulting sample goes all the way down to the sensitivity limit of the RASS-BSC catalogue of $f = 3 \times 10^{-13}$ erg/s/cm^2 (see Table 2). As a result, we can estimate the expected number of TDE candidates in our sample from the number of candidates, N_0, found by Donley et al. (2002) as follows:

$$N \simeq N_0 \times \frac{S}{S_0} \times \left(\frac{f}{f_0}\right)^{-3/2}, \quad (7)$$

where S/S_0 is the ratio of the sky areas covered by the two studies and f/f_0 is the ratio of the corresponding limiting fluxes. This equation is approximate since it disregards reddening of the distant objects and assumes a simple power-law (with a slope of -3/2) $\log N$—$\log S$ distribution, with both of these assumptions being somewhat inaccurate (see e.g. Khabibullin, Sazonov, & Sunyaev 2014).

The sky coverage of the *XMM-Newton* observations corresponding to the 3XMM-DR4 catalogue is 794 deg^2, i.e. almost 2% of the whole sky, which is 1/9th of the area covered by the *ROSAT* pointed observations (Donley et al. 2002). Given $N_0 = 6$ candidates (including SBS 1620+545 with a hard X-ray spectrum and two candidates with AGN signatures) found by Donley et al. (2002) at $|b| > 30°$, we find from the above equation $N = 11.5$, roughly in agreement with the number (eight) of TDE candidates

Figure 9. DSS image (2'x2') of the region around 1RXS J235424.5-102053

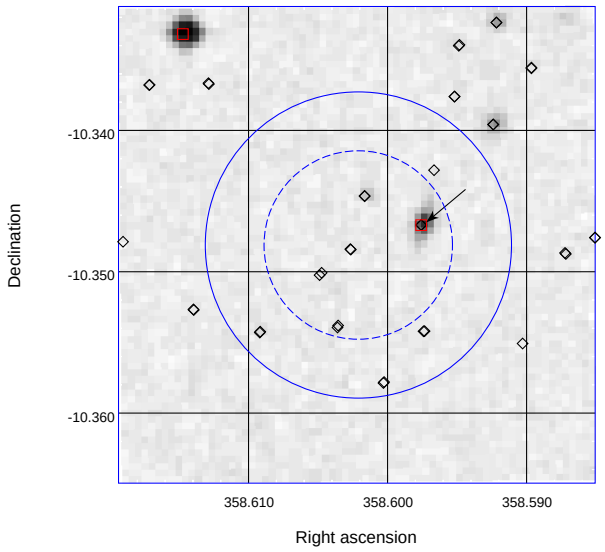

we actually found in our study (as well as with the number anticipated by Donley et al. 2002 for such a *XMM-Newton*-RASS cross-correlation study).

However, as we showed in Section 3, three of our candidates (1RXS J002048.5-253823, 1RXS J005626.3-010615 and 1RXS J215101.5-302852) are likely to be high-amplitude AGN flares, and yet another one (1RXS J101326.2+061202) might be associated with an intense flare from a K-star. Finally, *three* candidates are broadly consistent with the expectations of the TDE scenario. Namely, 1RXS J114727.1+494302, 1RXS J130547.2+641252 and 1RXS J235424.5-102053 can be associated with sufficiently bright galaxies without signatures of luminous AGN, although we cannot exclude that 1RXS J235424.5-102053 is a spurious RASS source. For the fourth source, 1RXS J112312.7+012858, a TDE association is also acceptable but an AGN association could not be rejected conclusively.

Thus, among our *eight* candidates, 3 or 4 could be associated with AGN, 1 with a flaring star and 2 to 4 with TDEs. Interestingly, Donley et al. (2002) found a similar proportion of candidates for AGN flares and TDEs, which supports the conclusion above that the numbers of TDEs found in these two studies are *broadly* consistent with each other.

4.2 TDE rate in the local Universe

The simple estimates presented above disregard a number of important points. First, by increasing the sensitivity of a survey, one gets the possibility not only to detect more distant TDE flares, but also flares at a later phase of their decay, i.e. 'older' ones at closer distances. Second, the problem in hand involves rather soft X-ray sources with the spectral maximum near or even below the *ROSAT* sensitivity range. This, along with the importance of the interstellar absorption in this energy range, makes the estimates quite sensitive to the cosmological reddening of the spectra. In addition, the non-cubic dependence of the comoving volume on the luminosity distance needs to be accounted for when dealing with redshifts ~ 0.15. Finally, the sky coverage of *XMM-Newton* observations is not completely independent of the positions of RASS-BSC sources, since some of them were the targets of *XMM-Newton* observations.

To estimate the last effect, we first find that $\sim 8\%$ of all RASS-BSC extragalactic ($|b| > 30^\circ$) sources have ever been observed by *XMM-Newton*, either on purpose or serendipitously, whereas the sky coverage of the 3XMM-DR4 catalogue is only 2% of that for the RASS (essentially the whole sky). However, the relative fraction of *XMM-Newton* targets among RASS-BSC sources should depend on the class of object of interest. As concerns the present study, which is aimed at non-extended, variable sources, the only potentially important source of bias might be associated with clusters of galaxies, which have often been targets of observations for *XMM-Newton*. Indeed, since clusters contain a lot of galaxies, they are expected to be cites of strongly increased TDE activity. However, since our study probes the Universe out to $z \sim 0.2$, an *XMM-Newton* ($\sim 15' \times 15'$) field of view randomly located on the sky will contain more galaxies than a rich cluster, hence there should be no significant bias due to *XMM-Newton* pointing at galaxy clusters. Moreover, the fact that a significant part of the XMM-DR4 catalogue is based on observations of fields containing galaxy clusters may in fact result in a decrease in the effective coverage for our study, since *ROSAT*'s rather poor angular resolution prevents finding TDE flares in the vicinity of cluster cores.

Indeed, only two out of eight candidates in our final sample of TDE candidates, namely, 1RXS J114727.1+494302 and 1RXS J130547.2+641252, prove to have been targets of *XMM-Newton* observations, while the others were observed serendipitously. Thus, the *XMM-Newton* sky coverage can indeed be considered almost independent of RASS-BSC sources when dealing with TDE candidates.

Following the treatment in Khabibullin, Sazonov, & Sunyaev (2014), we assume now some characteristic shape for the light curve, spectrum and energetics of a TDE. Specifically, given $M_{bh} = 5 \times 10^6 M_\odot$, one expects a blackbody spectrum with $\kappa T_{bb} \simeq 50$ eV, the peak bolometric luminosity (assumed to be equal to the Eddington limiting luminosity) $L_0 \simeq 7 \times 10^{44}$ erg/s and the characteristic light curve time-scale $\tau_{Edd} \simeq 0.19$ yr (see Sections 2.1 and 2.2 in Khabibullin, Sazonov, & Sunyaev 2014 and references therein). The original spectrum will be modified by interstellar absorption both in the host galaxy and along the line-of-sight in our Galaxy. The median value of the Galactic HI column density for the sources in our sample is $N_H^0 \simeq 2.7 \times 10^{20} \mathrm{cm}^{-2}$ (see Table 2). The absorption due to the gas in the host galaxy could be of the same order but is poorly known (see e.g. the comparison of the net N_H value found by the fitting the X-ray spectra for one of our candidates, RBS 1032, to the corresponding Galactic absorption in that direction, Ghosh et al. 2006). Just for convenience, we adopt the host's absorption column density $N_H^{host} \simeq 2.3 \times 10^{20}$ cm^{-2}, so that the net column density $N_H \simeq 5 \times 10^{20}$ cm^{-2} (note that the Galactic absorption is imposed in the observer's reference frame, while the host's absorption in the rest frame of the TDE).

In order to calculate the limiting redshift for a TDE flare at which it could still be identified as a bright *ROSAT* source (i.e. with the count rate more than 0.05 cts/s), we performed a `fakeit` simulation using *XSPEC* (Dorman & Arnaud 2001) and the *ROSAT* response matrix as provided by the NASA's High Energy Astrophysics Science Research Archive Center (HEASARC)[16]. Assuming $M_{bh} = 5{\times}10^6 M_\odot$, the limiting redshift turns out to be $z_{lim} \simeq 0.18$

[16] https://heasarc.gsfc.nasa.gov/docs/rosat/rosgof.html

[17]. This can be considered the characteristic depth of our sample. Using this value and repeating the calculation presented in Section 4.1 of (Khabibullin, Sazonov, & Sunyaev 2014), we finally can estimate the TDE rate in the local Universe at $\mathcal{R} \simeq 8(4)\times10^{-7}$ Mpc^{-3} yr^{-1}, assuming that there are *four (two)* 'true' TDEs in our sample (see Table 4 and the discussion above).

This estimate should still be regarded as an upper limit, since we cannot yet conclusively identify as a TDE any of our four best candidates. Given the volume density of inactive galaxies of 2×10^{-2} Mpc^{-3}, our estimate translates to a rate $R \simeq 3 \times 10^{-5}$ of TDEs yr^{-1} per galaxy, which falls in between the estimate of Donley et al. (2002), 9.1×10^{-6} yr^{-1} per galaxy, and the one by Esquej et al. (2008), 2.3×10^{-4} yr^{-1} per galaxy. One can also try to predict this rate by combining equation (29) in Wang & Merritt (2004) for the expected dependence of the TDE rate on M_{BH} and σ with the well-known $M_{BH} - \sigma$ relation (e.g. Ferrarese & Ford 2005; Gültekin et al. 2009): $R \sim 3 \times 10^{-4}$ yr^{-1} per galaxy. The fact that the rates derived from the cited observations are all well below this prediction could be due to an underestimation of the mean intrinsic column density (as discussed by Sembay & West 1993; see also the related discussions in Donley et al. 2002 and Esquej et al. 2008), as well as due to uncertainties in the average properties of nuclear stellar clusters in nearby galaxies.

We should also mention attempts to systematically search for TDEs using long observations of predefined samples of galaxies, in particular clusters of galaxies (Cappelluti et al. 2009; Maksym, Ulmer, & Eracleous 2010; Maksym et al. 2013). Although such studies have found just a few TDE candidates, their results are also consistent with our estimated TDE rate of a few$\times10^{-5}$ yr^{-1} per galaxy (Maksym et al. 2013).

5 CONCLUSIONS

We presented the results of a systematic search for tidal disruption events by looking for large (more than ten-fold) flux drops for sources from the *ROSAT* Bright Source Catalogue during serendipitous observations performed 10–20 years later by *XMM-Newton*. Besides a number of highly variable persistent X-ray sources (AGN, CVs and stars), we have found up to *four* sources that could be associated with TDEs in non-active galaxies. Specifically, *three* candidates are broadly consistent with the expectations of the TDE scenario: 1RXS J114727.1+494302, 1RXS J130547.2+641252 and 1RXS J235424.5-102053, although the last object may be a spurious RASS source due to contamination by diffuse cluster emission. For 1RXS J112312.7+012858, a TDE association is also acceptable, but an AGN origin cannot be ruled out conclusively either. This implies the mean TDE rate $R \sim 3 \times 10^{-5}$ yr^{-1} per galaxy within the surveyed volume, which is broadly consistent with previous estimates.

Due to the high sensitivity achieved in serendipitous observations by *XMM-Newton*, our sample of TDE candidates is significantly deeper than the previous ones by Donley et al. (2002) and Esquej et al. (2008). For this reason, it enables probing the TDE rate out to a larger redshift, up to $z \sim 0.18$ (making some reasonable assumptions about typical TDEs). The consistency of the TDE rate found in our work with the estimates based on the previous studies, which probed the more local Universe, tentatively suggests no significant evolution of the TDE rate between $z = 0$ and $z \sim 0.2$. The TDE rate derived here is also consistent with the rough estimate made for TDEs in clusters of galaxies (e.g. Maksym et al. 2013), thus indicating no dependency on the large-scale environment either.

We stress again that, in the absence of direct evidence, all of our suggested TDEs should still be regarded as TDE candidates. Further investigation of these sources is required (first of all, by means of optical spectroscopy) in order to confirm the absence of nuclear activity and to determine the distance to the host galaxy. Such information would help improve our estimate of the TDE rate. In addition, distance information would make it possible to estimate the peak luminosities of the TDEs and thus to constrain the masses of the SMBHs in the TDE host galaxies.

A by-product of our study is a small sample of high-amplitude AGN flares. More detailed studies of these sources could provide some insights into the mechanisms of AGN variability and consequently the physics of accretion onto SMBHs (like in the case of WPVS 007, Grupe et al. 2013).

ACKNOWLEDGEMENTS

The authors thank the anonymous referee for a number of useful suggestions. We would also like to thank Rodion Burenin for critical and stimulating discussions. IK acknowledges the support of the Dynasty Foundation. The research made use of grant RFBR 13-02-01365.

[17] In fact, the limiting redshift depends on M_{bh} only slightly in the range from $10^6 M_\odot$ to $10^7 M_\odot$, see the corresponding discussion in Khabibullin, Sazonov, & Sunyaev (2014).

REFERENCES

Abazajian K., et al., 2004, AJ, 128, 502
Agüeros M. A., et al., 2009, ApJS, 181, 444
Aird J., et al., 2010, MNRAS, 401, 2531
Anderson S. F., et al., 2003, AJ, 126, 2209
Anderson S. F., et al., 2007, AJ, 133, 313
Appenzeller I., et al., 1998, ApJS, 117, 319
Ayal S., Livio M., Piran T., 2000, ApJ, 545, 772
Bade N., et al., 1998, A&AS, 127, 145
Bauer F. E., Condon J. J., Thuan T. X., Broderick J. J., 2000, ApJS, 129, 547
Beuermann K., Thomas H.-C., Reinsch K., Schwope A. D., Trümper J., Voges W., 1999, A&A, 347, 47
Binney J., Merrifield M., 1998, "Galactic Astronomy", Princeton University Press
Blackburn, J. K. 1995, in ASP Conf. Ser., Vol. 77, Astronomical Data Analysis Software and Systems IV, ed. R. A. Shaw, H. E. Payne, and J. J. E. Hayes (San Francisco: ASP), 367.
Böhringer H., et al., 2004, A&A, 425, 367
Bower G. C., Metzger B. D., Cenko S. B., Silverman J. M., Bloom J. S., 2013, ApJ, 763, 84
Brandt W. N., Hasinger G., 2005, ARA&A, 43, 827
Burwitz V., Reinsch K., Beuermann K., Thomas H.-C., 1997, A&A, 327, 183
Cappelluti N., et al., 2009, A&A, 495, L9
Cenko S. B., et al., 2012, ApJ, 753, 77
Donley, J. L., Brandt, W. N., Eracleous, M., & Boller, T. 2002, ApJ, 124, 1308
Cohen M., Wheaton W. A., Megeath S. T., 2003, AJ, 126, 1090
Dorman, B., & Arnaud, K. A. 2001, Astronomical Data Analysis Software and Systems X, 238, 415
Esquej, P., Saxton, R. D., Komossa, S., et al. 2008, A&A, 489, 543
Evans C. R., Kochanek C. S., 1989, ApJ, 346, L13
Favata, F., Micela, G. 2003, SSRv, 108, 577
Ferrarese L., Ford H., 2005, SSRv, 116, 523
Gezari S., et al., 2009, ApJ, 698, 1367
Gezari S., 2012, EPJWC, 39, 3001
Ghosh K. K., Suleymanov V., Bikmaev I., Shimansky S., Sakhibullin N., 2006, MNRAS, 371, 1587
Greiner J., Schwarz R., Hasinger G., Orio M., 1996, A&A, 312, 88
Greiner J., Danner R., Bade N., Richter G. A., Kroll P., Komossa S., 1996, A&A, 310, 384
Grupe D., Beuerman K., Mannheim K., Thomas H.-C., Fink H. H., de Martino D., 1995, A&A, 300, L21
Grupe D., Komossa S., Scharwächter J., Dietrich M., Leighly K. M., Lucy A., Barlow B. N., 2013, AJ, 146, 78
Gültekin K., et al., 2009, ApJ, 698, 198
Gurzadian V. G., Ozernoi L. M.,1981, A&A, 95, 39
Haakonsen C. B., Rutledge R. E., 2009, ApJS, 184, 138
Hickox R. C., Markevitch M., 2006, ApJ, 645, 95
Hudaverdi M., Kunieda H., Tanaka T., Haba Y., Furuzawa A., Tawara Y., Ercan E. N., 2006, PASJ, 58, 931
Jarrett T. H., et al., 2011, ApJ, 735, 112
Kalberla P. M. W., Burton W. B., Hartmann D., Arnal E. M., Bajaja E., Morras R., Pöppel W. G. L., 2005, A&A, 440, 775
Khabibullin I., Sazonov S., Sunyaev R., 2014, MNRAS, 2549
Komossa, S. 2002, Reviews in Modern Astronomy, 15, 27
Komossa S., 2012, EPJWC, 39, 2001
Lasker B. M., et al., 2008, AJ, 136, 735
Läsker R., Ferrarese L., van de Ven G., Shankar F., 2014, ApJ, 780, 70
Lin D., Carrasco E. R., Grupe D., Webb N. A., Barret D., Farrell S. A., 2011, ApJ, 738, 52
Maccacaro T., Gioia I. M., Wolter A., Zamorani G., Stocke J. T., 1988, ApJ, 326, 680
Mahony E. K., Croom S. M., Boyle B. J., Edge A. C., Mauch T., Sadler E. M., 2010, MNRAS, 401, 1151
Maksym W. P., Ulmer M. P., Eracleous M., 2010, ApJ, 722, 1035
Maksym W. P., Ulmer M. P., Eracleous M. C., Guennou L., Ho L. C., 2013, MNRAS, 435, 1904
McGlynn T. A., et al., 2004, ApJ, 616, 1284
Merloni A., et al., 2012, arXiv, arXiv:1209.3114
Muerset U., Wolff B., Jordan S., 1997, A&A, 319, 201
Panessa F., Bassani L., 2002, A&A, 394, 435
Phinney E. S., 1989, IAUS, 136, 543
Pounds K. A., et al., 1993, MNRAS, 260, 77
Rees, M. J. 1988, Nature, 333, 523
Rutledge R. E., Brunner R. J., Prince T. A., Lonsdale C., 2000, ApJS, 131, 335
Saxton R. D., Read A. M., Esquej P., Komossa S., Dougherty S., Rodriguez-Pascual P., Barrado D., 2012, A&A, 541, A106
SDSS-III Collaboration, et al., 2012, ApJS, 203, 21
Sembay S., West R. G., 1993, MNRAS, 262, 141
Shakura, N. I., & Sunyaev, R. A. 1973, A&A, 24, 337
Singh K. P., et al., 1995, ApJ, 453, L95
Skrutskie M. F., et al., 2006, AJ, 131, 1163
Stern D., et al., 2012, ApJ, 753, 30
Stone N., Sari R., Loeb A., 2013, MNRAS, 435, 1809
Strubbe, L. E., & Quataert, E. 2009, MNRAS, 400, 2070
Taylor M. B., 2005, ASPC, 347, 29
Thomas H.-C., Beuermann K., Schwope A. D., Burwitz V., 1996, A&A, 313, 833
Thomas H.-C., Beuermann K., Reinsch K., Schwope A. D., Truemper J., Voges W., 1998, A&A, 335, 467
Trümper J., et al., 1991, Natur, 349, 579
Ulmer, A. 1999, ApJ, 514, 180
van Velzen S., et al., 2011, ApJ, 741, 73
Verbunt F., Bunk W. H., Ritter H., Pfeffermann E., 1997, A&A, 327, 602
Véron-Cetty M.-P., Véron P., 2006, A&A, 455, 773
Voges W., et al., 1996, rftu.proc, 637
Voges W., et al., 1999, A&A, 349, 389
Wang J., Merritt D., 2004, ApJ, 600, 149
Watson M. G., et al., 2009, A&A, 493, 339
Watson M. G., et al., 2013, "The XMM-Newton Serendipitous Survey. VII. The Third XMM-Newton Serendipitous Source Catalogue", in preparation.
Wright E. L., et al., 2010, AJ, 140, 1868
Zickgraf F.-J., et al., 1997, A&AS, 123, 103
Zimmermann H.-U., Boller T., Döbereiner S., Pietsch W., 2001, A&A, 378, 30